Biomechanical simulation of atrophy in MR images

Castellano Smith, Andrew, Crum, William, Hill, Derek, Thacker, Neil, Bromiley, Paul

Andrew D. Castellano Smith, William R. Crum, Derek L. G. Hill, Neil A. Thacker, Paul A Bromiley, "Biomechanical simulation of atrophy in MR images," Proc. SPIE 5032, Medical Imaging 2003: Image Processing, (15 May 2003); doi: 10.1117/12.480412

SPIE.

Event: Medical Imaging 2003, 2003, San Diego, California, United States

Biomechanical simulation of atrophy in MR images

Andrew D. Castellano Smith[*a], William R. Crum[a], Derek L.G. Hill[a],
Neil A. Thacker[b], Paul A. Bromiley[b]
[a]Division of Imaging Sciences, Kings College London, UK,
[b]Division of Imaging Science & Biomedical Engineering, University of Manchester, UK.

ABSTRACT

Progressive cerebral atrophy is a physical component of the most common forms of dementia - Alzheimer's disease, vascular dementia, Lewy-Body disease and fronto-temporal dementia. We propose a phenomenological simulation of atrophy in MR images that provides gold-standard data; the origin and rate of progression of atrophy can be controlled and the resultant remodelling of brain structures is known. We simulate diffuse global atrophic change by generating global volumetric change in a physically realistic biomechanical model of the human brain. Thermal loads are applied to either single, or multiple, tissue types within the brain to drive tissue expansion or contraction. Mechanical readjustment is modelled using finite element methods (FEM). In this preliminary work we apply these techniques to the MNI brainweb phantom to produce new images exhibiting global diffuse atrophy. We compare the applied atrophy with that measured from the images using an established quantitative technique. Early results are encouraging and suggest that the model can be extended and used for validation of atrophy measurement techniques and non-rigid image registration, and for understanding the effect of atrophy on brain shape.

Keywords: dementia, atrophy, modelling, FEM, atlas, MRI

1.INTRODUCTION

It has been known for many years that progressive cerebral atrophy is a physical component of the most common forms of dementia (AD, vascular dementia, Lewy-Body disease and frontotemporal dementia) which account for 90% of cases and affect more than 700,000 people in the UK. Cognitive decline and rate of atrophy in AD are strongly associated, reflecting the effects of neuronal damage at the cellular level[1]. The regional distribution of cellular damage is due to different pathologies and leads to different spatial patterns of atrophy in different dementias[2]. Other causes of neuronal damage are also increasingly being recognised to be associated with atrophy. Progressive atrophy is a diffuse cellular loss which does not simply scale the brain but changes positions of both internal and external tissue boundaries, opens up sulcal spaces and permits thinly connected structures like the temporal lobes to displace independently of the rest of the brain. Diffuse atrophy may affect the size, appearance and configuration of neuroanatomical structures. A new generation of disease-specific therapeutic agents[3] means that it is important to achieve a firm diagnosis at the earliest possible stage. However definitive differential diagnosis relies on histological analyses which cannot be performed *in vivo*. Cognitive testing, the patterns of atrophy visible on MR images of the brain and the rate of atrophy progression contribute to diagnosis, especially in early stages of disease.

A number of image analysis techniques have evolved to estimate total cerebral atrophy. The most powerful (BBSI[4] and SIENA[5]) use serial imaging in conjunction with precise three-dimensional image registration allowing changes over time in the individual to be tracked. Other techniques used for establishing regional patterns of atrophy in groups of patients (eg RAVENS[6], Voxel Based Morphometry[7]) are being applied in clinical studies[8]. Most atrophy measurement techniques require calibration but it is extremely difficult to validate their results against controllable but realistic test data and questions about their efficacy remain. Brain images displaying simulated atrophy of known magnitude and location are a potentially valuable resource for calibrating and validating atrophy measurement techniques. Global cerebral atrophy has previously been simulated by globally scaling images to effect a global

[*] Andrew.Castellano-Smith@kcl.ac.uk; phone +44 (0) 20 7955 2721; fax +44 (0) 20 7955 4532; www-ipg.umds.ac.uk

reduction in brain-tissue volume accompanied by an unrealistic reduction in CSF volume (usually CSF-spaces expand to fill areas once occupied by atrophying tissue)[9]. Localised scaling has been used to validate measurement of atrophy in much smaller structures such as the hippocampus[10], the right precentral gyrus and the left superior temporal gyrus[6]. Validation of the group-wise techniques is more difficult still and requires whole groups of test data which should exhibit both a range of features seen in the normal population and a range of disease-specific features. These experiments have not been performed to our knowledge. For some applications such as analysis of group differences between different dementias the absolute amount of atrophy is less important than the ability to distinguish patient and control groups. However in the future when atrophy measurement supports diagnosis and disease-specific therapeutic intervention, both the absolute rate and location of atrophy will become important.

The complexity of microscopic disease processes and their relationship with brain morphology at a voxel level is daunting. Never-the-less it is possible to simulate atrophy in different tissue compartments or in different neuro-anatomical structures as a phenomenological process guided by expert clinical knowledge. The consequent biomechanical readjustment of structures can be modelled using conventional physics-based techniques. Ultimately such a combined model can be guided by, or validated against statistical models of atrophy derived from measurements in well-defined patient groups.

In this paper we present details of a phenomeological model of brain atrophy incorporated into a finite element framework which includes (a) reduction in brain tissue volume, (b) expansion of ventricular CSF volume (c) biomechanical readjustment of tissue. The model is applied to simulated Magnetic Resonance Images of an example brain to produce new brain images exhibiting varing degrees of atrophy. The actual volumetric change as determined from the warped finite-element mesh is compared with that desired and with that measured directly from the new images. Drawbacks and possible improvements to the technique are discussed and the value of simulated atrophied brain images to other areas of medical image analysis is noted.

2. METHODS

Atlas Images and Atlas Mesh Construction

The MNI brainweb phantom[11] (http://www.bic.mni.mcgill.ca/brainweb/) was used as our atlas brain model. Segmentations of the major tissue compartments in the simulated brain images are publically available. Surface models of the outer brain surface (grey-matter/CSF boundary) and the ventricular surfaces were extracted from the brainweb images using a modified marching cubes technique[12] before being smoothed and decimated to remove very small edges and very small triangular facets using the "evolver" software package (http://www.susqu.edu/facstaff/b/brakke/evolver/evolver.html). This smoothing and decimation process has been shown to preserve salient features of surface shape, whilst providing a reduction in the number of facets making up the model surface[13]. A commercial FEM package, ANSYS[14] (http://www.ansys.com) was used to construct the interior volumes of these surfaces and to generate a combined volume. Tetrahedral elements were used to mesh this multi-component volume so as to preserve the internal boundaries within the object - in this case the ventricular surfaces, whilst producing a continuous mesh across that surface. The final mesh contains 45974 nodes and 33801 tetrahedral elements. The Young's modulus of the tissues were set to $4x103NM^{-2}$ for white matter, and $8x103NM^{-2}$ for grey matter, with Poisson's ratio of 0.495 for near incompressibility[15]. All tissues were modelled as linear elastic solids using 10-noded tetrahedral elements (the "solid187" element in ANSYS). Since atrophy is small in relation to the total brain volume, and the strains therefore relatively small, it is reasonable to use a small displacement linear elastic model.

Simulation of atrophy

Biomechanical modelling techniques are commonly used in medicine to model the mechanical response of biological systems to a set of forces. Modelling atrophy within a FEM framework is not an obvious application. However the macroscopic effects of atrophy on the brain are two-fold. Firstly, there are effects on the volumes of the different tissue compartments and/or anatomical structures eg the temporal lobes may reduce in volume and the ventricles may increase in volume. Secondly there are effects of biomechanical remodelling where atrophy can significantly increase cortical sulcal volume and the volume of CSF surrounding structures such as the temporal-lobes. This can result in readjustment of the relative positioning of structures which means that the common "rigid-body" assumption applied to the brain no-

longer applies. Ideally a principled model of disease processes at a cellular level would be used to drive the progression of atrophy in the brain tissue compartments. At present the disease mechanisms which result in atrophy are not fully understood and the computational requirements for modelling these processes in sufficient detail are impractical. Therefore in this work we adopt a pragmatic approach and use a phenomenological model of atrophy which captures the essential characteristics of the process. Specifically we assume that atrophy is a diffuse, gradually progressive and continuous process. These assumptions are not restrictive and still allow spatio-temporal variations in atrophy to be explored. Within the FEM framework atrophy can be simulated by applying a positive or negative thermal load to the different tissue compartments in the model. Thermal loading induces a uniform expansion or shrinking force in a given tissue type by associating with each tissue type a suitable coefficient of thermal expansion and then applying a uniform temperature to the whole mesh. The coefficient of thermal expansion, ALPX, used by ANSYS is related to expansion and contraction as follows:

$$ALPX = 1 - \sqrt[3]{(1 - VolExpansion)} \text{ where } VolExpansion = \frac{\Delta V(t)}{V(t_{ref})} \qquad (1)$$

In equation 1, $V(t)$ represents the length of a material at temperature t and $V(t_{ref})$ is the length at a reference temperature t_{ref}. Then *VolExpansion* is the desired fractional volumetric change. Subsequent mechanical readjustment is modelled by the FEM. The FEM solution is used to produce an atrophied brain image by interpolating the displacements calculated at each node in the FEM mesh to give a displacement field specifying the displacement of each voxel in the image matrix.

Experiments

Two experiments were performed in this initial investigation. First we explored the parameter-space of simulated atrophy on the T1-weighted phantom data by applying a range of thermal loads to the GM and CSF tissue compartments. The thermal loads were calculated to produce volumetric changes consistent with those observed in dementia patients involved in serial scanning studies. The deformation induced in the finite-element mesh was then used to warp the brain image to simulate the appearance of atrophy. The actual volume changes induced in the mesh were computed exactly and compared with those predicted. The second experiment involved estimating atrophy directly from the images using an existing technique[16] which quantifies the age-corrected volume of cerebrospinal fluid in a standard anatomical space. This technique coregisters the images to a standard coordinate system using the rigid coregistration technique in the TINA machine vision software package[17]. For this work, binary masks of the CSF compartment were available for use but when applied to patient data the CSF compartment would be extracted from the images. The lower extents of the CSF masks to be included in the measurement were defined by drawing a line in the midsagittal section parallel to the horizontal axis that passed through the junction of the calvarium and the tentorium cerebelli; this defined the inferior limit of the measurement space. All other limits were defined as the maximal extent of the CSF space and the total volume of the CSF in the measurement space was recorded for each simulated image. This technique usually estimates CSF volume over 12 standardised regional compartments but for the purposes of these initial experiments the total CSF volume change was simply compared with that measured from the warped mesh.

3. RESULTS

The results of systematically varying the thermal loads applied to the CSF and GM compartments can be seen in Figure 1a. A single axial slice is shown for all combinations of the thermal loads. The % applied GM change is shown along the top of the page and the % applied CSF change is shown down the page. Changes from one panel to the next are quite subtle but more obvious changes can be seen visually by comparing more widely separated rows and columns. Figure 1b is formatted identically to figure 1a but each panel contains a subtraction image showing the difference between the warped and unwarped images which makes significant shifts in tissue boundaries easier to see.

Figure 2a shows the % volume change of CSF measured from the deformed mesh as a function of the change predicted from the applied thermal loads in the absence of any loads applied to the GM compartment. The system shows a highly linear response with an attenuation of the predicted change of about 20%. Figure 2b shows the % volume change of GM measured from the deformed mesh compared with the change predicted in the absence of loads applied to the CSF compartment. Again an extremely good linear response is seen with an attenuation of only 5%.

The situation becomes more complicated when loads are applied to both tissue compartments simultaneously. Figure 3a shows measured CSF volume change compared with predicted as before but for each applied CSF load, the full range of GM loads as shown in figure 1 are applied. It can be seen that this results in a variation in the measured CSF volume change. For any particular GM load, the CSF response remains linear but the attenuation varies. In some extreme cases, the CSF volume actually decreases. A similar trend can be seen in figure 3b where the affect of CSF loads on measured GM volume change can be seen. Again the measured GM volume change remains a remarkably linear function of the applied volume change for constant CSF load.

Figure 4a shows the CSF volume change measured from the warped images as a function of the change measured in the deformed images with no GM loads applied. This is a key result which links volumetric change in the finite element mesh with change in voxel appearance in the resulting images. Again the response is very linear but the attenuation of voxel-measured compared with mesh-measured is over 50%. This initially surprising result is explained in the next section. Figure 4b shows CSF volume changes measured from the images when simultaneous GM loads are applied.

4. CONCLUSIONS

This model of atrophy is extremely simple but results in atrophied images of a surprisingly realistic appearance. The two major points of discussion relate to discrepancies between measured atrophy (either from the mesh or the resulting images) and predicted atrophy. The small attenuation seen in figures 2a and 2b can be atttributed to the fact that all tissues are being modelled as linear elastic solids. Therefore, when the CSF compartment is expanding under a thermal load there will be an elastic force resisting that expansion from the brain tissue compartments even if no thermal loads are being applied to them. The thermal loads have been calculated assuming no forces resisting the volume change and therefore the measured volume change tends to be smaller than predicted. When thernal loads are applied to both CSF and GM then both compartments will change volume until the elastic forces balance and equilibrium is reached. This results in the spread of measured values for tissue volume change seen in figures 3a and 3b. The large discrepancy seen in figure 4a and 4b has a different explanation. The finite element brain model used in this work does not currently model extra-cortical CSF but the estimates of CSF volume change derived from the images are calculated over the entire cranial cavity. In future work we intend to extend the simulation model to include this CSF (see below) and possibly apply the atrophy measurement technique to a masked ventricular region of the images.

The shortcomings of this modelling technique are many yet the results are surprisingly good. At present the most obvious problem is that the thermal loads applied to the CSF and tissue compartments are uncoupled. It is a natural next step to parameterise the changes by a single parameter which balances atrophy of tissue with expansion of CSF. A more subtle short-coming which may ultimately be more important is that contracting or expanding parts of a single image may change the local texture or scale-space properties which could impact on the suitability of such images in certain testing arenas. There is room for improvement in the brain model by (a) increasing the mesh resolution, (b) adding a “skull” boundary condition and improving the treatment of extra-cortical CSF (c) more detailed labelling and explicitly incorporating midbrain structures. In this work we have simulated global diffuse atrophy as might be found in Alzheimer’s Disease but in the future it should be reasonably straight-forward to simulate the regional atrophy found in some other dementias (eg fronto-temporal) or to investigate more focal changes in structures such as the hippocampus which are hypothesised to occur in early disease.

In the experiments described in this paper, atrophy has been simulated on the brain images for which the finite element mesh was developed. It is straightforward to individualise this mesh to other brain images using non-rigid image registration as has already been done to model neurosurgical change[18]. This makes possible the generation of cohorts of simulated atrophic images which might find use in testing and validation of group-analysis techniques such as Voxel Based Morphometry. Alternatively, serial sets of images of individuals can be produced to simulate disease progression and test and validate quantitative methods such as BBSI and SIENA for measuring atrophy from images.

As the prevelance and sophistication of non-rigid registration techniques increases, together with the use of analysis techniques which depend on them, the availability of good validation strategies becomes vitally important. The simulation techniques described in this paper are a simple step in the right direction which have applications spanning

validation of registration, segmentation and atrophy measurement and a role to play in the understanding of how diffuse processes affect brain shape.

5. REFERENCES

1. N.C. Fox , R.I. Scahill , W.R. Crum and M.N. Rossor, "Correlation between rates of brain atrophy and cognitive decline", Neurology 52, 1687-1689, 1999.
2. D. Chan, N.C. Fox, R.I. Scahill, W.R. Crum, J.L. Whitwell, G. Leschziner, A. Rossor, J.M. Stevens, L. Cipolotti and M.N. Rossor, "Patterns of temporal lobe atrophy in semantic dementia and Alzheimer's disease", Annals of Neurology 49 (4), 433-442, 2001.
3. Elan Pharmaceuticals Inc. "A randomised, double-blinded, safety, tolerability and pilot efficacy study of AN1792(QS-21) in patients with mild to moderate Alzheimer's disease", 2002.
4. N.C. Fox and P.A. Freeborough, "Brain atrophy progression measured from registered serial MRI: validation and application to Alzheimer's disease.", Magn Reson Imaging 7(6), 1069-75, 1997.
5. S. Smith, Y.Zhang, M. Jenkinson, J. Chen, P. Matthews, A. Federico and N. De Stefano, "Accurate, robust and automated longitudinal and cross-sectional brain change analysis.", NeuroImage 17 (1), 479-489, 2002.
6. C. Davatzikos, A. Genc, D. Xu, and S.M. Resnick, "Voxel-Based Morphometry Using the RAVENS Maps: Methods and Validation Using Simulated Longitudinal Atrophy", NeuroImage 14, 1361-1369, 2001.
7. J. Ashburner and K.J. Friston, "Voxel based morphometry – the methods", Neuroimage 11, 805-821, 2000.
8. J.C. Baron, G. Chételat, B. Desgranges, G. Perchey, B. Landeau, V. de la Sayett and F. Eustache, "In Vivo Mapping of Gray Matter Loss with Voxel-Based Morphometry in Mild Alzheimer's Disease", NeuroImage 14(2), 298-309, 2001.
9. P.A. Freeborough and N.C. Fox, "The boundary shift integral: An accurate and robust measure of cerebral volume changes from registered repeat MRI", IEEE Transactions. on Medical Imaging, 16(5), 623-629, 1997.
10. W.R. Crum, R.I. Scahill and N.C. Fox, "Automated hippocampal segmentation by regional fluid registration of serial MRI: Validation and application in Alzheimer's disease", NeuroImage 13 (5), 847-855, 2001.
11. D.L. Collins, A.P. Zijdenbos, V. Kollokian, J.G. Sled, N.J. Kabani, C.J. Holmes, A.C. Evans, "Design and Construction of a Realistic Digital Brain Phantom", IEEE Transactions on Medical Imaging, 17 (3), 463-468, 1998.
12. W.E.Lorensen, H.E.Cline, "Marching Cubes: A high resolution 3d surface construction algorithm", Computer Graphics 32(4):163-169, 1987.
13. AD Castellano-Smith, "The human brain: from shape to function", PhD Thesis, University of London, 1999.
14. ANSYS Inc. 275 Technology Drive, Canonsburg, PA 5317, USA.
15. H.Takizawa, K.Sugiura, M.Baba, J.D.Miller, "Analysis of intracerebral hematoma shapes by numerical computer simulation using the finite element method", Neurol Med Chir (Tokyo), 34(2):65-69, 1994.
16. N.A. Thacker, A.R. Varma, D. Bathgate, S. Stivaros, J.S. Snowden, D. Neary and A.Jackson, "Dementing Disorders : Volumetric Measurement of Cerebrospinal Fluid from Pathologic Findings – Feasibility Study", Radiology 224, 278-285, 2002.
17. N.A. Thacker, A. Lacey, E. Vorkurka, X.P. Zhu, K.L. Li and A. Jackson, "TINA an Image Analysis and Computer Vision Application for Medical Imaging Research". Proc. ECR, s566, Vienna, 1999.
18. A.D. Castellano Smith, T. Hartkens, J.A. Schnabel, R. Hose, H. Liu, W. Hall, C. Truwit, D.J. Hawkes and D.L.G. Hill, "A registration based mesh construction technique for finite element models of brains", In Proc. SPIE Medical Imaging 2002: Image Processing 4683, 538-549, 2002.

6. ACKNOWLEDGEMENTS

William R. Crum and Paul A. Bromily are funded by the EPSRC-MRC Medical Images and Signals IRC. This work is a product of the collaborative environment and opportunities afforded us by this research programme.

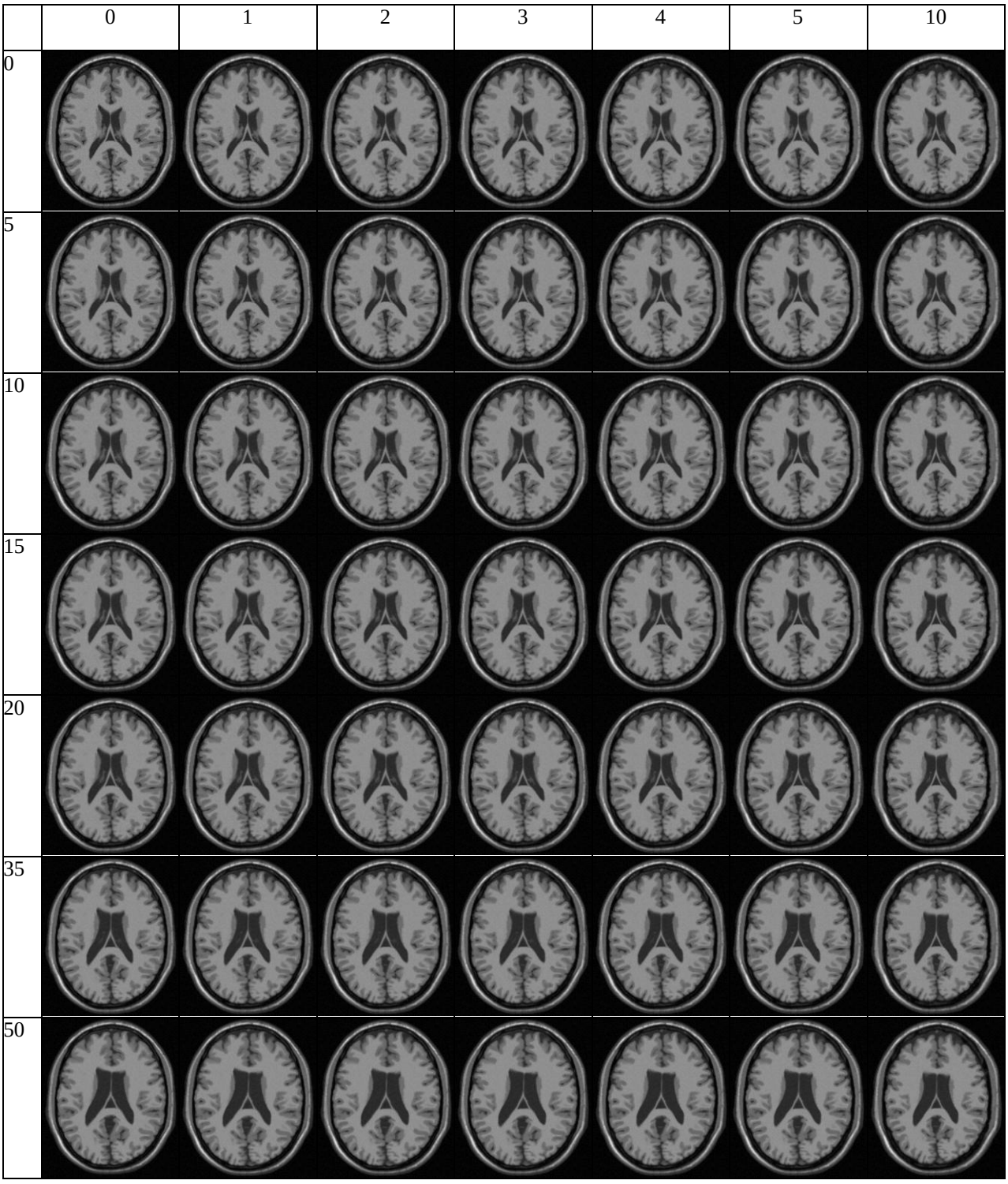

Figure 1a : Example slices exhibiting simulated atrophy. The row values are % CSF volume change predicted and the column values are % GM volume change predicted.

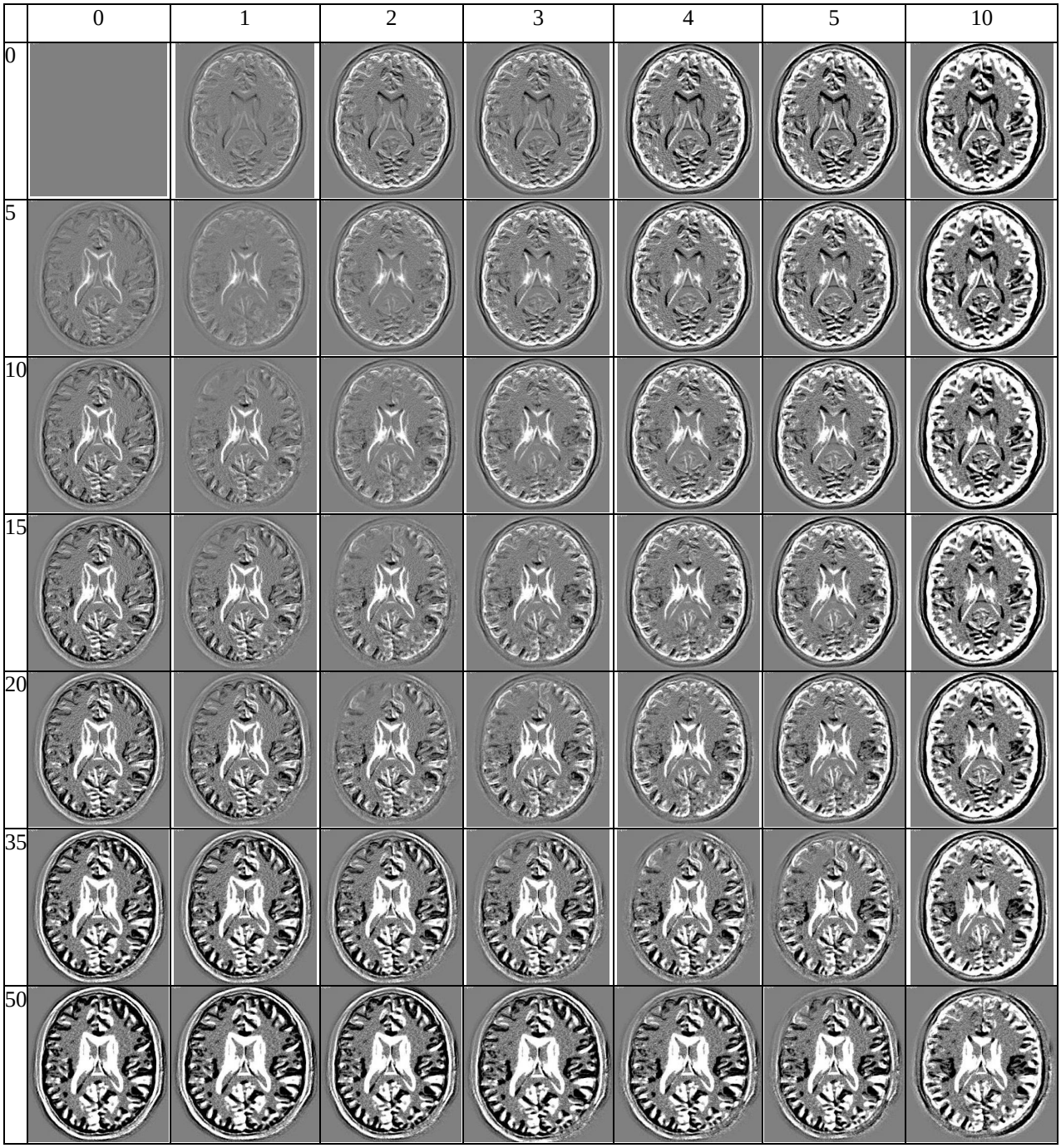

Figure 1b : Example slices exhibiting simulated atrophy. The row values are % CSF volume change predicted and the column values are % GM volume change predicted.

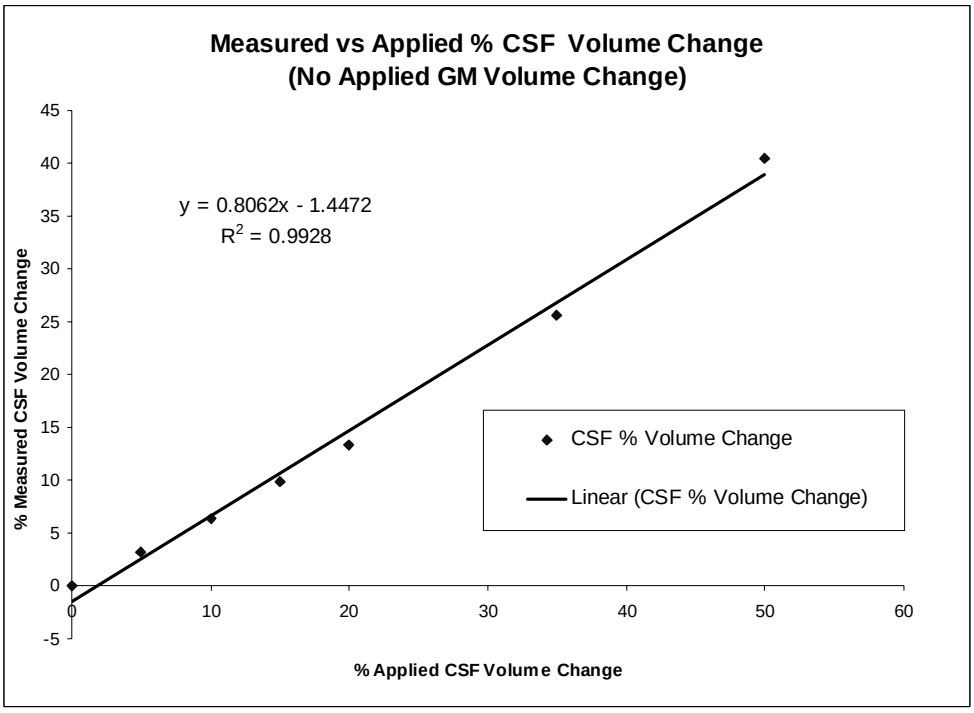

Figure 2a: Comparison of CSF change induced in the mesh with that predicted.

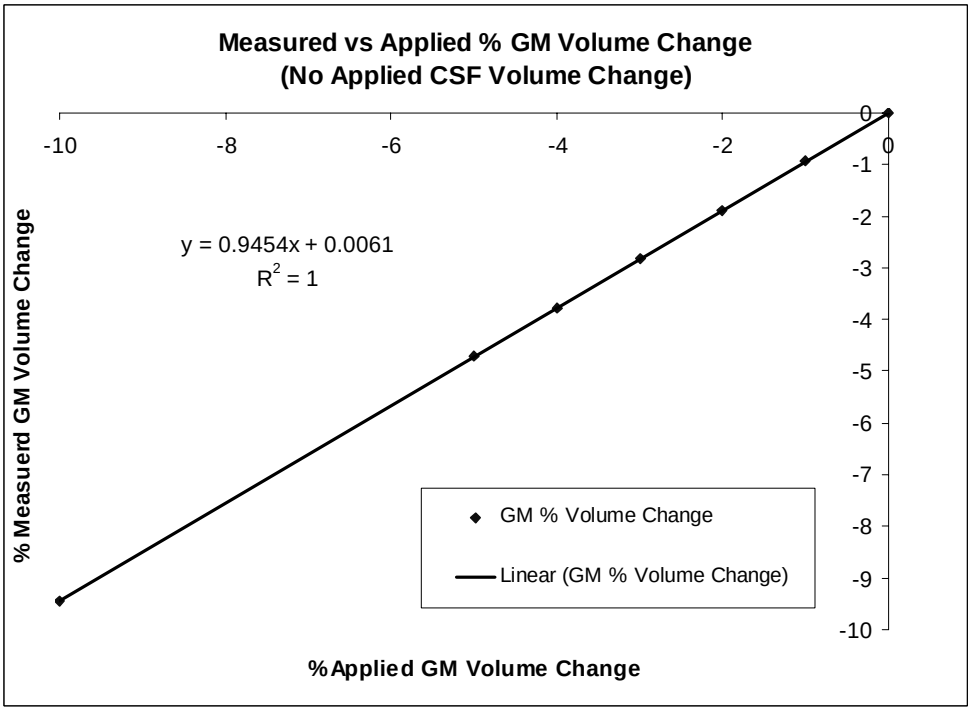

Figure 2b: Comparison of GM change induced in the mesh with that predicted.

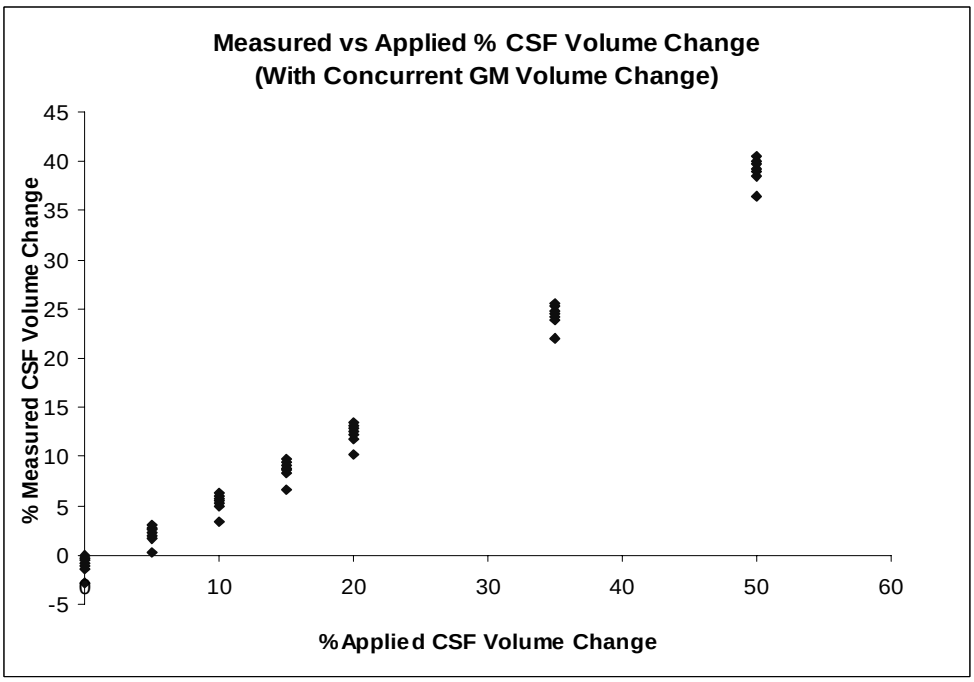

Figure 3a: Comparison of CSF change induced in the mesh with that predicted. Concurrent GM changes were applied.

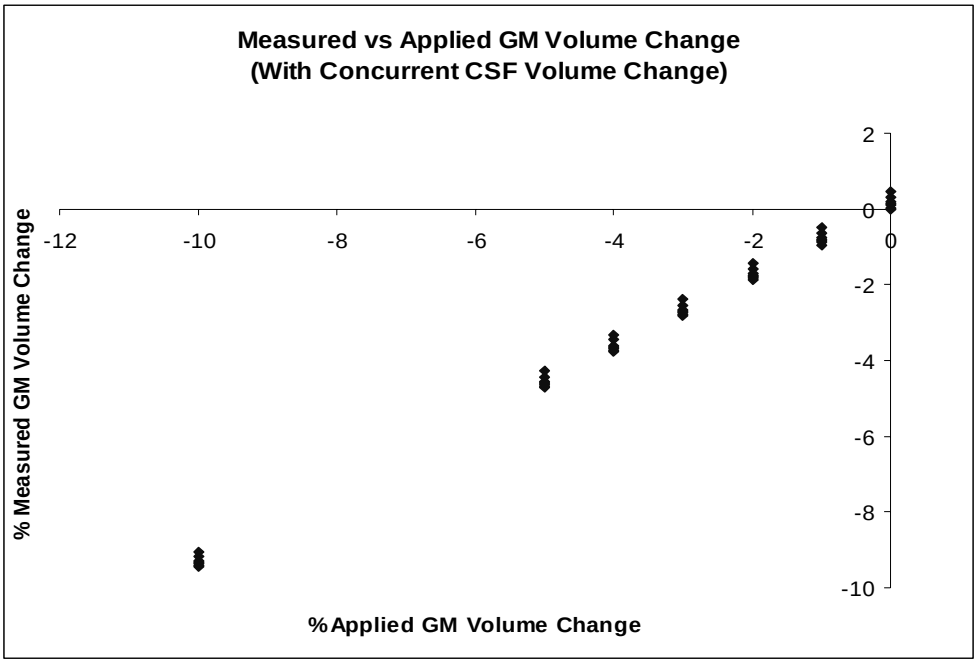

Figure 3b: Comparison of GM change induced in the mesh with that predicted. Concurrent CSF changes were applied.

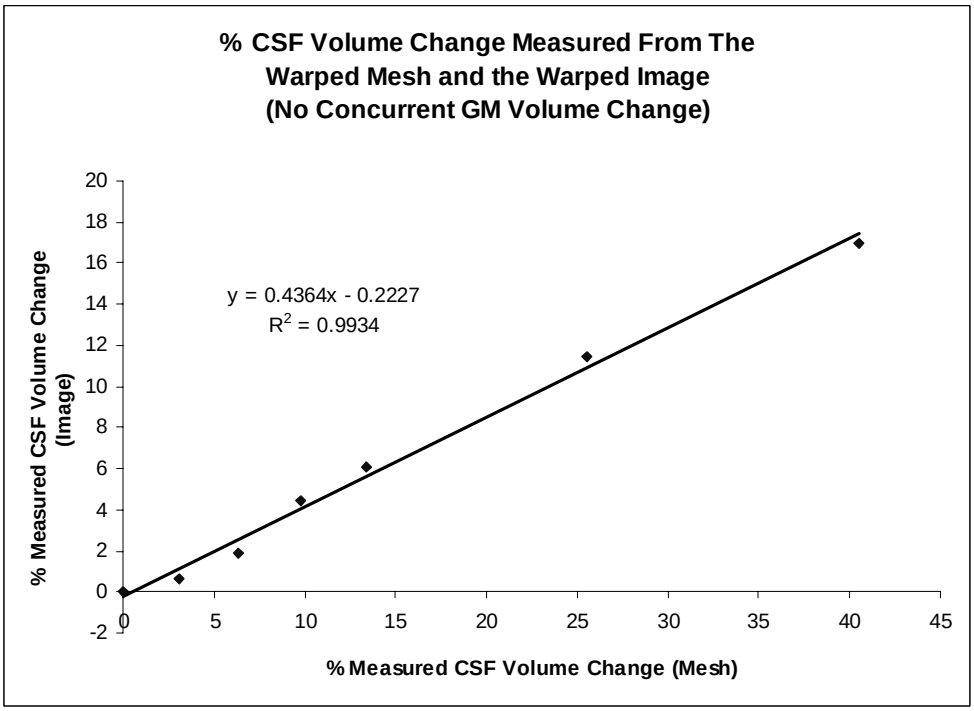

Figure 4a: Comparison of CSF change measured in the images with that in the mesh.

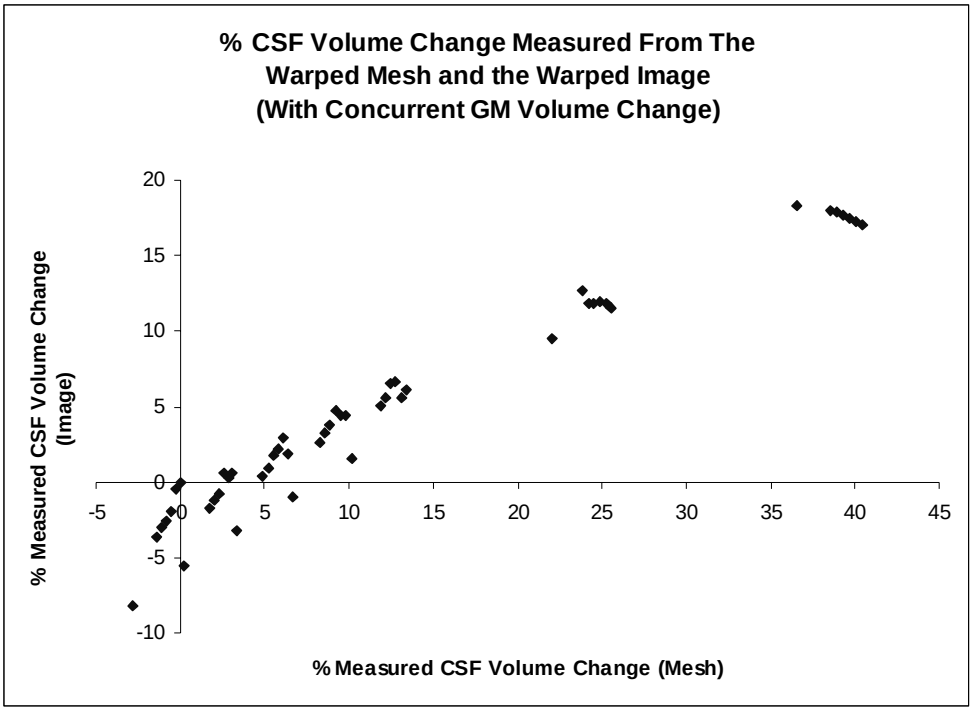

Figure 4b: Comparison of CSF change measured in the images with that in the mesh. Concurrent GM changes were applied.